Journal of the Serbian Chemical Society
JSCS@tmf.bg.ac.rs • www.shd.org.rs/JSCS

J. Serb. Chem. Soc. *87* (5) 575–587 (2022)
JSCS–5542

Original scientific paper
Published 23 March 2022

Theoretical calculation of newly synthesized tetrazolopyrimidine derivatives as a potential corrosion inhibitor

ERDEM ERGAN[1]*, NURULLAH SEKER[2], BEGUM CAGLA AKBAS[3] and ESVET AKBAS[2]

[1]*Department of Property Protection and Security, Van Security Vocational School, Van Yuzuncu Yil University, 65080, Van- Turkey,* [2]*Department of Chemistry, Faculty of Science, Van Yuzuncu Yil University, 65080 Van-Turkey and* [3]*Faculty of Pharmacy, University of Inonu, Malatya, Turkey*

(Received 19 April, revised 14 July, accepted 4 August 2021)

Abstract: In this work, we wanted to define a general and comprehensive strategy for the synthesis of tetrazolo[1,5-*a*]pyrimidine derivatives. For this purpose, we obtained new tetrazolo[1,5-*a*]pyrimidine molecules *via* the mercury-promoted desulfurization reaction, including hydrolysis, cyclizations, and eliminations. All of the molecules were characterized by FT-IR, ^{1}H-NMR, ^{13}C--NMR, and elemental analysis. On the other hand, the potentials of compounds as corrosion inhibitors were calculated at B3LYP/6-31G (d, p) level *via* density functional theory (DFT).

Keywords: desulfurization; DFT; characterization; quantum chemical studies; sodium azide.

INTRODUCTION

Corrosion is the deterioration of metal by reacting with chemicals or the environment. Corrosive solutions are used in many industrial applications. Acid solutions widely used in industry, especially in the cleaning process cause a significant mass loss on the surface.[1–3] Many methods are used to prevent corrosion. One of the methods of preventing corrosion is to use protective materials. Organic compounds are also one of the important materials used as protective materials.

The organic compounds containing π-bonds, phosphorus, sulfur, oxygen, and nitrogen as well as aromatic rings in their structure interacts with the metal surface and show high inhibition property.[4] The compounds containing both nitrogen and sulfur can provide excellent inhibition, compared with compounds containing only nitrogen or sulfur.[5] Generally, a strong interaction causes higher

* Corresponding author. E-mail: erdem_ergan@hotmail.com
https://doi.org/10.2298/JSC210419067G

inhibition efficiency, the inhibition increases in the sequence O < N < S.[6] It has been reported to increase the inhibition efficiency in general that compounds containing heteroatoms (S, N and O) with free electron pairs, delocalized π-electron aromatic rings, molecular weight, alkyl chains, and generally as a result of the existence of substituted groups. Compounds with π-bonds also generally exhibit good inhibitive properties due to the interaction of π-orbital with the metal surface.[7]

It is preferred that the compounds used for corrosion inhibiting purposes are not harmful to nature. For this reason, pyrimidine derivatives have attracted great attention due to their less environmentally damaging properties.[8] However; studies on pyrimidine are limited despite their ease of availability and corrosion inhibition properties.

Pyrimidine derivatives are among the important class of organic compounds. They exhibit broad biochemical effects due to the activity of nitrogen atoms in the ring and carbon atoms in the C2/C4/C6 position.[9] Due to these properties, pyrimidine derivative compounds are used as active ingredients in drugs such as uramustine, piritrexim, isethionate, tegafur, floxuridine, fluorouracil, cytarabine and methotrexate.[10] Pyrimidine derivatives are promising concerning corrosion inhibition.[11]

Experimental techniques like the weight-loss method, electrochemical impedance spectroscopy (*EIS*), potentiodynamic polarization, *etc.*, have been used to understand the corrosion process and its inhibition.[12,13] Although experiments mostly are time-consuming, costly, and lacking in explaining the mechanism of inhibition of the corrosion.[14,15] Thus, the quantum chemical calculation method was endorsed as a potent and easy tool to reduce the cost and time and can help in the interpretation of the experimental findings.[16,17]

Heakal *et al.*[18] used quantum chemical calculations to determine the structural and electronic properties of imidazole-pyrimidine-based new ionic compounds. They compared the theoretical inhibition yields of the compounds prepared in this way. Molecules chosen as inhibitors must be capable of donating electrons to the empty *d*-orbital of the metal and also be suitable for forming anti-feedback bonds. Pyrimidine compounds have these properties. Therefore, pyrimidine derivatives are expected to be excellent corrosion inhibitors at the industrial level.[19]

Quantum chemical calculations (QCCs) are widely used to find the corrosion inhibition reactivity of organic molecules. The effectiveness of an inhibitor can be related not only to its spatial molecular structure but also its molecular electronic structure. According to frontier orbital theory, the reaction of reactants mainly occurred on highest occupied molecular orbital (HOMO) and lowest unoccupied molecular orbital (LUMO), and the formation of a transition state is due to an interaction between the frontier orbitals of the reactants. So, it was imp-

ortant to investigate the distribution of HOMO and LUMO for the exploration of the inhibition mechanism.

The difference between E_{LUMO} and E_{HOMO} energies is called the energy gap (ΔE). It was generally acknowledged that low values of ΔE will provide good inhibition efficiency because the energy for removing an electron from the last occupied orbital will be low. For the theoretical calculation of the inhibitory effect of a molecule, it is necessary to know the ionization potential (I), the electron affinity (A), the chemical hardness-softness (S), the global electrophilicity index (ω), the interaction between the transmitted electron fraction index (ΔN), the interaction between back donations and non-linear optical (NLO) properties. All these values were calculated according to Shojaie *et al.* [20] using DFT-based QCCs in the Gaussian 09 software.[21]

EXPERIMENTAL

Chemicals and instruments

All chemicals and solvents used in the experiments were assured from Turkey representative of Sigma Aldrich and Fluka (Buchs, Switzerland). All reactions were monitored by thin-layer chromatography (TLC). TLC plates were based on silica gel 60 F254 aluminum plates with a 0.2 mm layer thickness (Merck Co., Darmstadt, Germany). The spots in TLC were determined by the UV lamp. Stuart (UK) SMP30 melting point apparatus was used to measure the melting points of the synthesized compounds. FT-IR spectra of compounds were measured in the range of 4000–400 cm^{-1} by using a Perkin Elmer Spectrum 100 FT-IR spectrometer (universal ATR sampling accessory). ^{1}H- and ^{13}C-nuclear magnetic resonance (NMR) spectra of compounds were measured in DMSO-d_6 by using a Bruker (Billerica, MA) AVANCDPX-400 MHz spectrometer at 400 and 100 MHz, respectively. Tetramethylsilane (TMS) was used as the internal reference. Elemental analyses were determined by using a Thermo Scientific (Pittsburgh, PA) Flash 2000 elemental analyzer. Full geometry optimizations of all molecules were performed using Gaussian09. The physical, analytical and spectral data for the compounds are given in the Supplementary material to this paper.

Synthesis

*(7-(4-(Methylthio)phenyl)-5-phenyl-4,7-dihydrotetrazolo[1,5-α]pyrimidin-6-yl)(phenyl) methanone (**6**)*. The mixture of (4-(4-(methylthio)phenyl)-6-phenyl-2-thioxo-1,2,3,4-tetrahydropyrimidin-5-yl)(phenyl)methanone (1 mmol),[22] sodium azide (2 mmol) and mercuric acetate (1 mmol) in acetic acid (5 mL) was stirred at 100 °C for 6 h. After completion of the reaction (monitored by thin-layer chromatography), the black sediment (HgS) was filtrated. Then water was added to the filtrate to give the crude product. It was recrystallized from ethyl alcohol.

*(7-(4-Hydroxyphenyl)-5-phenyl-4,7-dihydrotetrazolo[1,5-α]pyrimidin-6-yl)(phenyl) methanone (**7**)*. 0.386 g (4-(4-hydroxyphenyl)-6-phenyl-2-thioxo-1,2,3,4-tetrahydropyrimidin-5-yl)(phenyl) methanone (1 mmol),[23] sodium azide (2 mmol) and mercuric acetate (1 mmol) in acetic acid (5 mL) was stirred at 100 °C for 6 h. After completion of the reaction (monitored by thin-layer chromatography), the black sediment (HgS) was filtrated. Then water was added to the filtrate to give the crude product. It was recrystallized from methyl alcohol.

*(7-(4-Methoxyphenyl)-5-phenyl-4,7-dihydrotetrazolo[1,5-α]pyrimidin-6-yl)(phenyl) methanone (**8**)*.[24] 1 mmol (4-(4-methoxyphenyl)-6-phenyl-2-thioxo-1,2,3,4-tetrahydropyrimidin-5-

-yl)(phenyl)methanone,[25] sodium azide (2 mmol) and mercuric acetate (1 mmol) in acetic acid (5 mL) was stirred at 100 °C for 6 h. After completion of the reaction (monitored by thin-layer chromatography), the black sediment (HgS) was filtrated. Then water was added to the filtrate to give the crude product. It was recrystallized from isopropyl alcohol.

*(5,7-Diphenyl-4,7-dihydrotetrazolo[1,5-α]pyrimidin-6-yl)(phenyl)methanone (**9**)*.[24] 1 mmol (4,6-diphenyl-2-thioxo-1,2,3,4-tetrahydropyrimidin-5-yl)(phenyl)methanone,[26] sodium azide (2 mmol) and mercuric acetate (1 mmol) in acetic acid (5 mL) was stirred at 100 °C for 6 h. After completion of the reaction (monitored by thin-layer chromatography), the black sediment (HgS) was filtrated. Then water was added to the filtrate to give the crude product. It was recrystallization from butyl alcohol.

RESULTS AND DISCUSSION

Synthesis

Recently, structures change associated with mercury-promoted desulfurization reactions, including hydrolysis, cyclizations, and eliminations, have been reported.[27,28] Because of the strong thiophilic affinity of Hg^{2+}, mercuric acetate was used in the design of formation for HgS. We devised a strategy in which the azido group would be formed by desulfurization of 3,4-dihydropyrimidine-2-thiones using Hg^{2+}. The addition of the Hg^{2+} ion-induced the N_3^- to attack the 2-C atom of pyrimidine, followed by the removal of HgS and the formation of intramolecular guanylation. Finally, a stable cyclic product tetrazolo[1,5-α]pyrimidines were formed through an irreversible desulfurization reaction, as depicted in Scheme 1.

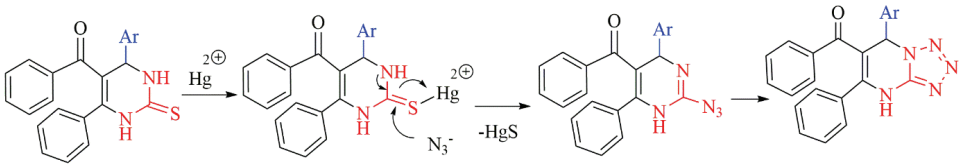

Scheme 1. Formation of tetrazolo[1,5-α]pyrimidines through an irreversible desulfurization reaction.

In this paper, we aimed to define a general and comprehensive strategy for the synthesis of tetrazolo[1,5-*a*]pyrimidine derivatives (Scheme 2).

We chose the reaction of compound **1** and sodium azide as a model reaction to optimize the reaction conditions. A series of experiments were performed to evaluate the feasibility of the formation of tetrazolo[1,5-α]pyrimidines. The results are shown in Table I. It can be said that compound **1**/NaN_3/mercuric(II) acetate (1:2:1) at 100 °C in acetic acid is the best result.

Analysis results of all synthesized compounds support the expected structure. Details of the analysis results are given in the Supplementary material. In addition to the structural analysis of the obtained compounds, the electronic properties were also calculated using computer calculation methods.

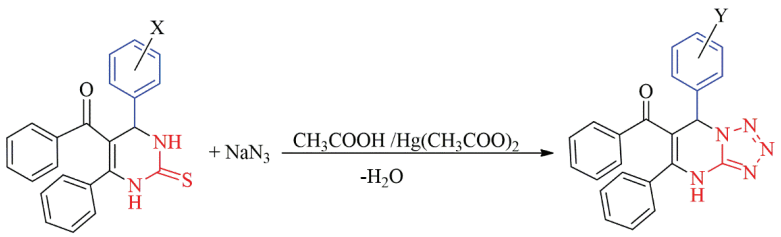

	X
1	4-SCH_3
2	4-OH
3	4-OCH_3
4	4-H

	Y
6	4-SCH_3
7	4-OH
8	4-OCH_3
9	4-H

Scheme 2. Desulfurization reaction for pyrimidine compounds.

TABLE I. Optimization of reaction conditions for compound **6**

Compound **1**:NaN_3:desulfurization reagent mole ratio	Solvent	Desulfurization reagent	T / °C	t / h	Yield, %
1:2:1	Acetic acid	Mercuric(II) acetate	25	10	–
1:2:1	Acetic acid	Mercuric(II) acetate	75	7	65
1:2:1	Acetic acid	Mercuric(II) acetate	100	6	85
1:2:1	Acetic acid	Mercuric(II) acetate	110	6	85
1:2:1	Methanol	Mercuric(II) acetate	65	6	60
2:4:1	Acetic acid	Mercuric(II) acetate	100	6	85
1:2:1	Acetic acid	Mercury(II) chloride	100	6	75
1:2:1	Acetic acid	Mercury(II) chloride	25	12	–

Computational analysis

Geometry optimizations of molecules were studied using Gaussian09. Calculations made DFT based on B3LYP and the 6-31G (d, p) orbital basis sets (Fig. 2).[21,29–31]

Quantum chemical parameters of synthesized compounds such as μ, I, A, χ, η, w, S, ΔN and $\Delta E_{\text{back donation}}$ were calculated according to Karzazi *et al.*[32] (Table II) using the Gaussian09 program. With this method, it is possible to predict the corrosion preventive effects of organic molecules.

The adsorption of the molecule to the metal surface causes the inhibitory effect. When the attachment occurs chemically, the ligand acts as an electron donor, and the metal acts as an electron acceptor (Fig. 3).

The inhibition effect of the molecule is related to the ground state geometry of the HOMO and LUMO structures (Fig. 4). The high HOMO region in the molecule acts as the favorite adsorption area due to its electron density.

Excellent corrosion inhibitors represented by organic compounds behaving, at the same time, on the one hand as electron donors to unoccupied d orbital of the metal surface to form coordinate covalent bonds, and on the other hand as the

acceptor of free electrons from the metal surface by using their antibonding orbitals to form feedback bonds. The LUMO energy level of molecules is the molecule's ability to accept electrons. When the LUMO energy level of the inhibitor molecule is lower, it is capable of accepting more electrons. The skill of the inhibitor to bind to the metal surface increases with increasing HOMO energy value and decreases LUMO energy value. Therefore, inhibitors with a lower E_{LUMO} value are more likely to be accepted onto the metal surface.

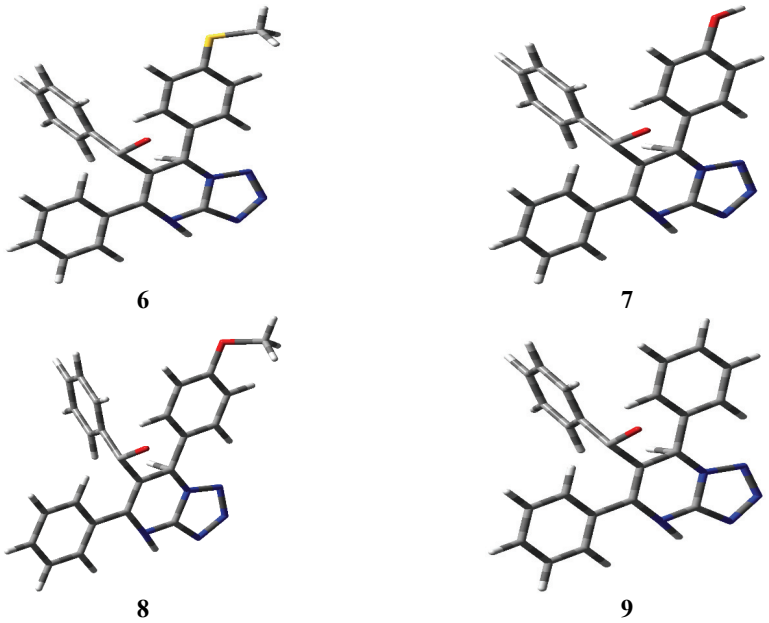

Fig. 2. Optimizations of all compounds.

TABLE II. The quantum chemical parameters for all compounds

Parameter	**6**	**7**	**8**	**9**
E_{HOMO} / eV	–4.9564	–5.5164	–5.5183	–6.1793
E_{LUMO} / eV	–3.4349	–3.4445	–3.4450	–1.9146
ΔE / eV	1.5214	2.0719	2.0733	4.2646
Ionization potential, eV	4.9564	5.5164	5.5183	6.1793
Electron affinity, eV	3.4349	3.4445	3.4450	1.9146
Chemical hardness, eV	0.7607	1.0359	1.0366	4.2647
Chemical softness, eV^{-1}	1.3146	0.9653	0.9646	0.2345
Electronegativity, eV	4.1956	4.4805	4.4815	4.0469
Transferred electrons fraction	1.8433	1.2161	1.2148	0.3463
Electrophilicity index	16.6809	12.9347	12.7732	52.437
Dipole moment, D[a]	5.0377	5.1767	5.1460	5.2688
$\Delta E_{back\ donation}$ / eV^{-1}	–0.1902	–0.2589	–0.2591	–1.0662

[a]1 D = 3.335×10^{30} C m

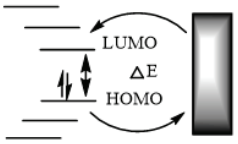

Fig. 3. Interaction of organic molecules with the metal surface.

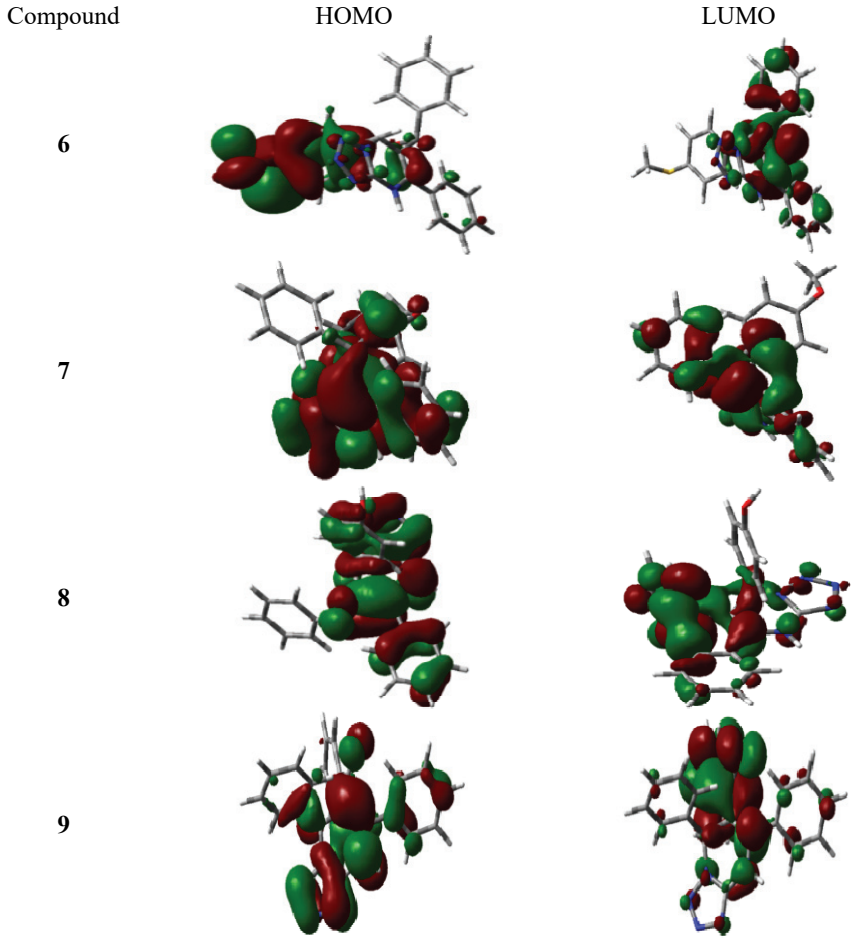

Fig. 4. HOMO and LUMO molecular orbitals.

The energy gap (ΔE) value indicates the difference between HOMO and LUMO energy levels. This value is an important parameter that shows the reactivity of the inhibitor molecule against adsorption on the metal surface. Low values of ΔE have been shown in previous studies to provide good inhibition.[33] A molecule with a low ΔE becomes more polarized and is generally associated with high chemical activity and low kinetic stability. These structures are called soft molecules.[34] In this study, ΔE values are listed as 9 > 8 > 7 > 6. As a result,

it can be said that molecule 6 can show good corrosion inhibitor performance (Table II).

The dipole moment (μ) of the molecule is an important parameter in determining the inhibition property. The increase in the dipole moment value increases the adsorption resolution.[35]

Chemical hardness (η) and softness (S) are other important properties used to measure the stability and reactivity of a molecule.[36,37] Molecule **6** with values of η = 0.7607 eV and softness S = 1.3146 eV will show the highest inhibition effect.

The fraction of electrons transferred (ΔN) values were also calculated (Table II). If $\Delta N < 3.6$, inhibition efficiency increases.[38–40] The global electrophilicity index (ω) and the $\Delta E_{\text{back donation}}$ values for the compounds demonstrate that compound **6** exhibit a good inhibitory effect (Table II).

Molecular electrostatic potentials (MEPs)

MEP provides information on reactive sites for electrophilic and nucleophilic attack and hydrogen bond interactions for compounds. MEPs were obtained at B3LYP/6-31+G (d,p) level for all compounds and are given in Fig. 5. The negative (red) regions of the MEP indicate electrophilic reactivity and the positive (blue) regions show nucleophilic reactivity.

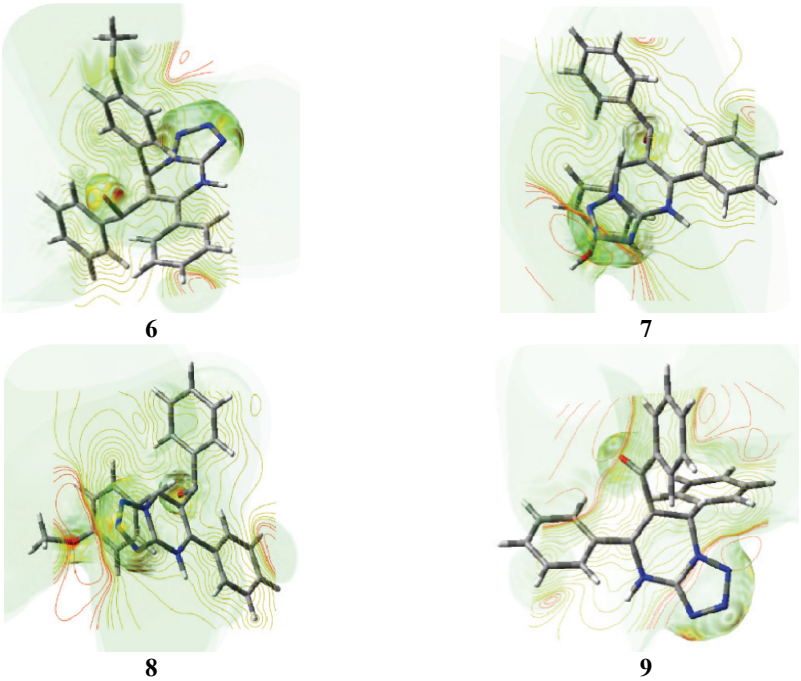

Fig. 5. MEPs of all molecules.

Non-linear optical (NLO) properties

NLO properties of compounds **6**–**9** were computed *via* the B3LYP/6-31+G (d,p) in the gas phase. Using the equations given below, the total dipole moment (μ_{tot}) by Eq. (1), mean polarizability (α_{tot}) by Eq. (2), and the average value of the first hyperpolarizability (β_{tot}) by Eq. (3) can be computed:

$$\mu_{tot} = \mu_x^2 + \mu_y^2 + \mu_z^2 \quad (1)$$

$$\alpha_{tot} = (\alpha_{xx} + \alpha_{yy} + \alpha_{zz})/3 \quad (2)$$

$$\beta_{tot} = [(\beta_{xxx} + \beta_{xyy} + \beta_{xzz})^2 + (\beta_{yyy} + \beta_{yxx} + \beta_{yzz})^2 + (\beta_{zzz} + \beta_{zxx} + \beta_{zyy})^2]^{0.5} \quad (3)$$

Calculated data and other components for the NLO are given in Table III.

TABLE III. Electric dipole moment μ, polarizability α_{tot} (10^{-33} esu*), and first hyperpolarizability β_{tot} (10^{-33} esu) for molecules **6**–**9** obtained by B3LYP level with the 6-31+g (d,p) basis set

Parameter	6	7	8	9
μ_x / D	1.7712	1.3178	1.8906	–0.4527
μ_y / D	0.1009	1.5123	0.3440	–1.3742
μ_z / D	–0.8864	–0.2771	–0.6759	–0.1959
μ_{tot}	17.1262	17.4944	17.5985	12.6132
α_{xx}	–64.7042	–57.1117	–63.0773	10.0268
α_{yy}	–61.7315	–60.0122	–59.3779	–12.1679
α_{zz}	–85.6467	–76.2526	–81.4938	2.1409
α_{tot}	–610.748	–556.879	–587.326	–0.0017
β_{xxx}	–24.2020	15.3040	–19.8924	–8.1824
β_{xyy}	21.5054	–9.2419	15.2620	–18.8274
β_{xzz}	28.5848	9.5182	28.2566	12.3043
β_{yyy}	8.9387	16.3674	12.4547	–55.1931
β_{yxx}	–2.7867	–4.2552	–8.6951	–6.3579
β_{yzz}	1.9177	22.7144	8.5003	–4.4225
β_{zzz}	–41.4856	–11.0272	–31.7697	1.0436
β_{zxx}	–7.3189	–28.6762	–29.1246	7.3687
β_{zyy}	–1.2435	–13.0927	0.2463	4.2575
β_{tot}	491.7667	562.7537	572.1984	594.120

Based on these data, it can be said that compounds with high dipole moment, high molecular polarizability, and high hyperpolarizability values will be more active. Based on the calculation results, it is seen that compounds **8** and **9**, which have the highest hyperpolarizability, will show more active NLO properties compared to other compounds.

In addition to these calculations, the intermolecular bond lengths, bond angles, and dihedrals of compound **6** were also calculated to serve as an example (Fig. 6 and Table IV).

* 1 esu = 3.336×10^{-10} C

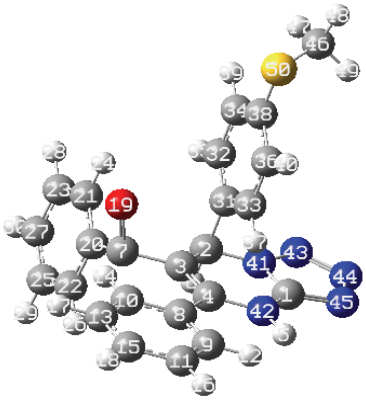

Fig. 6. The atom numbering for molecule **6**.

TABLE IV. Computed data are of selected bond lengths, angles, and dihedral angles for compound **6**

Bond	Bond length, Å	Bond angle, º	Dihedral angle, °
C(4)(3,2,1)	1.3899631	121.1386464	0.0026262
C(7)(3,2,1)	1.5400001	119.1112575	–179.998045
O(19)(7,3,2)	1.4300001	109.4712206	–90.0048931
H(5)(1,4,3)	2.1650737	56.7832079	179.994403
N(41)(2,1,4)	1.3803306	30.5550539	179.9931916
N(42)(1,41,2)	1.3802752	120.4036192	–0.0121285
N(43)(41,2,1)	1.4575035	132.5559472	179.9923687
N(44)(43,41,2)	1.4076826	108.1755697	–179.9890161
N(45)(44,43,41)	1.4071737	109.5727945	–0.0030415
C(46) (38,36,33)	2.3355950	131.6261913	–138.3953821
S(50)(46,38,36)	1.4300001	35.2500004	–84.4007167

CONCLUSION

The new tetrazolo[1,5-*α*]pyrimidine compounds were obtained by reaction of pyrimidine compounds with sodium azide. The structures of all molecules were determined by spectroscopic methods such as FT-IR, ^{1}H/^{13}C-NMR, and elemental analysis. The theoretical corrosion inhibition potentials of the compounds were investigated at the B3LYP/6-31G (d,p) level using density functional theory (DFT). In addition, molecular electrostatic potential maps and nonlinear optical (NLO) properties of the compounds were calculated theoretically. According to calculations, compound **6** is considered to be used as a good potential inhibitor for corrosion.

SUPPLEMENTARY MATERIAL

Additional data and information are available electronically at the pages of journal website: https://www.shd-pub.org.rs/index.php/JSCS/article/view/10683, or from the corresponding author on request.

Acknowledgement. This work was supported by the VanYYU, Project No: FYL-2018--7181.

ИЗВОД

ТЕОРИЈСКА ИЗРАЧУНАВАЊА НОВОСИНТЕТИСАНИХ ДЕРИВАТА ТЕТРАЗОЛОПИРИМИДИНА КАО ПОТЕНЦИЈАЛНИХ ИНХИБИТОРА КОРОЗИЈЕ

ERDEM ERGAN[1], NURULLAH SEKER[2], BEGUM CAGLA AKBAS[3] и ESVET AKBAS[2]

[1]*Department of Property Protection and Security, Van Security Vocational School, Van Yuzuncu Yil University, 65080, Van- Turkey,* [2]*Department of Chemistry, Faculty of Science, Van Yuzuncu Yil University, 65080 Van-Turkey и* [3]*Faculty of Pharmacy, University of Inonu, Malatya, Turkey*

У овом раду дефинисана је општа и свеобухватна стратегија за синтезу тетразоло[1,5-α]пиримидинских деривата. Добијени су нови тетразоло[1,5-α]пиримидински молекули у реакцији десулфуризације потпомогнуте живом, укључујући хидролизу, циклизацију и елиминацију. Сви молекули су окарактерисани са FT-IR, ^{1}H-NMR, ^{13}C--NMR и елементалном анализом. Са друге стране, потенцијали једињења као инхибитора корозије су израчунати на B3LYP/6-31G (d,p) нивоу теоријом функционала густине (DFT).

(Примљено 19. априла, ревидирано 14. јула, прихваћено 4. августа 2021)

REFERENCES

1. M. Lagrene, B. Mernari, M. Bouanis, M. Traisnel, F. Bentiss, *Corrosion Sci.* **44** (2002) 573 (https://doi.org/10.1016/S0010-938X(01)00075-0)
2. A. Yurt, S. Ulutas, H. Dal, *Appl. Surf. Sci.* **253** (2006) 919 (https://doi.org/10.1016/j.apsusc.2006.01.026)
3. S. Şafak, B. Duran, A. Yurt, G. Türkoğlu, *Corros. Sci.* **54** (2012) 25 (https://doi.org/10.1016/j.corsci.2011.09.026)
4. S. Shahabi, P. Norouzi, M. R. Ganjali, *Int. J. Electrochem Sci.* **10** (2015) 2646 (https://citeseerx.ist.psu.edu/viewdoc/download?doi=10.1.1.668.6592&rep=rep1&type=pdf)
5. J. Aljourani, M. A. Golozar, K. Raeissi, *Mater. Chem. Phys.* **121** (2010) 320 (https://doi.org/10.1016/j.matchemphys.2010.01.040)
6. A. Chetouani, A. Aouniti, B. Hammouti, N. Benchat, T. Benhadda, S. Kertit, *Corros. Sci.* **45** (2003) 1675 (https://doi.org/10.1016/S0010-938X(03)00018-0)
7. R. T. Loto, C. A. Loto, A P. I. Popoola, M. Ranyaoa, *Int. J. Phys. Sci.* **7** (2012) 2697 (https://www.researchgate.net/publication/313580988_Pyrimidine_derivatives_as_environmentally-friendly_corrosion_inhibitors_A_review)
8. K. Rasheeda, V. D. P. Alva, P. A. Krishnaprasad, S. Samshuddin, *Int. J. Corros. Scale Inhib*. **7** (2018) 48 (http://ijcsi.pro/papers/pyrimidine-derivatives-as-potential-corrosion-inhibitors-for-steel-in-acid-medium-an-overview/)
9. H. Dansena, H. J. Dhongade, K. Chandrakar, *Asian J. Pharm. Clin. Res*. **8** (2015) 171 (https://webcache.googleusercontent.com/search?q=cache:luNzlxY0zn8J:https://innovareacademics.in/journals/index.php/ajpcr/article/download/6283/2710+&cd=2&hl=tr&ct=clnk&gl=tr)
10. T. P. Selvam, C. R. James, P. V. Dniandev, S. K. Valzita, *Research in Pharm*. **2** (2012) 01 (https://updatepublishing.com/journal/index.php/rip/article/view/271)
11. M. Abdallah, E. A. Helal, A. S. Fouda, *Corros. Sci.* **48** (2006) 1639 (https://doi.org/10.1016/j.corsci.2005.06.020)

12. D-Q. Zhang, Q-R. Cai, X-M. He, L-X. Gao, G-D. Zhou, *Mater. Chem. Phys.* **112** (2008) 353 (https://doi.org/10.1016/j.matchemphys.2008.05.060)
13. M. A. Amin, M. M. Ibrahim, *Corros. Sci.* **53** (2011) 873 (https://doi.org/10.1016/j.corsci.2010.10.022)
14. N. A. Wazzan, I. Obot, S. Kaya, *J. Mol. Liq.* **221** (2016) 579 (https://doi.org/10.1016/j.molliq.2016.06.011)
15. B. Usman, I. Jimoh, B. A. Umar, *Appl. J. Environ. Eng. Sci.* **5** (2019) 66 (https://www.researchgate.net/publication/332195552_Theoretical_study_of_2_-3_4-dihydroxyphenyl_chroman-3_5_7-triol_on_corrosion_inhibition_of_mild_steel_in_acidic_medium)
16. Y. Atalay, F. Yakuphanoglu, M. Sekerci, D. Avcı, A. Başoğlu, *Spectrochim. Acta, A* **64** (2006) 68 (https://doi.org/10.1016/j.saa.2005.06.038)
17. E. E. Ebenso, T. Arslan, F. Kandemirli, N. Caner, I. Love, *Int. J. Quantum Chem*. **110** (2010) 1003 (https://doi.org/10.1002/qua.22249)
18. F. E. T. Heakal, S. A. Rizk, A. E. Elkholy, *J. Mol. Struct.* **1152** (2018) 328 (https://doi.org/10.1016/j.molstruc.2017.09.079)
19. E. Akbas, E. Yildiz, A. Erdogan, *J. Serbian Chem. Soc.* **85** (2020) 481 (https://doi.org/10.2298/JSC190326081A)
20. F. Shojaie, N. M. Baghini, *Int. J. Ind. Chem.* **6** (2015) 297 (https://doi.org/10.1007/s40090-015-0052-x)
21. *Gaussian 09, Revision E.01,* Gaussian, Inc., Wallingford, CT, 2009 (http://gaussian.com/g09citation/)
22. E. Akbas, E. Ergan, E. Sahin, S. Ekin, M. Cakir, Y. Karakus, *Phosphorus Sulfur Silicon Relat. Elem.* **194** (2019) 796 (https://doi.org/10.1080/10426507.2018.1550489)
23. E. Akbas, A. Levent, S. Gumus, M. R. Sumer, I. Akyazi, *Bull. Korean Chem. Soc.* **31** (2010) 3632 (https://doi.org/10.5012/bkcs.2010.31.12.3632)
24. E. Akbas, S. Celik, E. Ergan, A. Levent, *J. Chem. Sci.* **131** (2019) 30 (https://doi.org/10.1007/s12039-019-1602-0)
25. E. Ergan, E. Akbas, A. Levent, E. Sahin, M. Konus, N. Seferoglu, *J. Mol. Struct.* **1136** (2017) 231 (https://doi.org/10.1016/j.molstruc.2017.02.001)
26. F. Aslanoglu, E. Akbas, M. Sonmez, B. Anil, *Phosphorus Sulfur Silicon Relat. Elem.* **182** (2007) 1589 (https://doi.org/10.1080/10426500701263554)
27. Y. K. Yang, K. J. Yook, J. Tae, *J. Am. Chem. Soc.* **127** (2005) 16760 (https://doi.org/10.1021/ja054855t)
28. K. C. Song, J. S. Kim, S. M. Park, K. C. Chung, S. Ahn, S. K. Chang, *Org. Lett.* **8** (2006) 3413 (https://doi.org/10.1021/ol060788b)
29. A. D. Becke, *J. Chem. Phys.* **96** (1992) 2155 (https://doi.org/10.1063/1.462066)
30. A. D. Becke, *J. Chem. Phys.* **98** (1993) 1372 (https://doi.org/10.1063/1.464913)
31. C. Lee, W. Yang, R. G. Parr, *Phys. Rev., B* **37** (1988) 785 (https://doi.org/10.1103/PhysRevB.37.785)
32. Y. Karzazi, M. E. A. Belghiti, A. Dafali, B. Hammouti, *J. Chem. and Pharm. Res*. **6** (2014) 689 (https://www.jocpr.com/abstract/a-theoretical-investigation-on-the-corrosion-inhibition-of-mild-steel-by-piperidine-derivatives-in-hydrochloric-acid-sol-2763.html)
33. H. Zarrok, A. Zarrouk, R. Salghi, H. Oudda, B. Hammouti, M. Assouag, M. Taleb, M. Ebn Touhami, M. Bouachrine, S. Boukhris, *J. Chem. Pharm. Res.* **4** (2012) 5056 (https://www.jocpr.com/articles/gravimetric-and-quantum-chemical-studies-of-14acetyl24chlorophenylquinoxalin14hylacetone-as-corrosion-inhibitor-for-carb.pdf)

34. T. T. Adejumo, N. V. Tzouras, L. P. Zorba, D. Radanovic, A. Pevec, S. Grubišic, D. Mitic, K. K. Andelkovic, G. C. Vougiokalakis, B. Cobeljic, I. Turel, *Molecules* **25** (2020) 4043 (https://doi.org/10.3390/molecules25184043)
35. X. Li, S. Deng, H. Fu, T. Li, *Electrochim. Acta* 54 (2009) 4089 (https://doi.org/10.1016/j.electacta.2009.02.084)
36. N. Caliskan, E. Akbas, *Mater. Corros.* **63** (2012) 231 (https://doi.org/10.1002/maco.201005788)
37. N. Caliskan, E. Akbas, *Mater. Chem. Phys.* **126** (2011) 983 (https://doi.org/10.1016/j.matchemphys.2010.11.051)
38. R. Hasanov, M. Sadikoglu, S. Bilgic, *Appl. Surf. Sci.* **253** (2007) 3913 (https://doi.org/10.1016/j.apsusc.2006.08.025)
39. F. Bentiss, M. Lagrenée, *J. Mater. Environ. Sci.* **2** (2011) 13 (https://www.jmaterenvironsci.com/Document/vol2/3-JMES-62-2011-Bentiss2.pdf)
40. P. Udhayakala, T. V. Rajendiran, S. Gunasekaran, *J. Advanced Sci. Res.* **3** (2012) 71 (http://eds.b.ebscohost.com/eds/pdfviewer/pdfviewer?vid=1&sid=85d1e953-13bc-4e39-94f0-6c41acdeacb8%40sessionmgr102).